AIAA JOURNAL
Vol. 30, No. 5, May 1992

Experimental Investigation of Supersonic Flow over Two Cavities in Tandem

Xin Zhang* and John A. Edwards†
University of Cambridge, Cambridge, England, United Kingdom

A study is presented on supersonic flow over two rectangular cavities arranged in tandem at Mach 1.5, 2.5, and 3.5. Both time-mean and unsteady aspects of the flowfields are examined. For the purposes of this paper, cavities are chosen in which the oscillatory properties are due either to a fluid resonant phenomenon or to a fluid dynamic phenomenon. These are defined as type A and type B cavities, respectively. At Mach 1.5 and 2.5, the flow in a type A cavity is found to be completely altered by a preceding type B cavity. When the type B cavity is preceded by another type B cavity, only the level of the unsteady pressures and the high frequency modes of the oscillation are affected. When type A cavity precedes a type B cavity, only small quantitative changes are noted in the oscillatory behavior. The influence of the spacing between the two cavities is also addressed.

Nomenclature

C_f = skin friction coefficient
D = depth of the cavity
f = frequency in Hz
H = boundary-layer shape parameter, δ^*/Θ
L = length of the cavity
M = Mach number
N = number of points used in Fourier transform
p = pressure
PSD = power spectral density, $10 \log_{10} sp/2N\omega$
Re = Reynolds number, $\rho_e U_e D/\mu_e$
sp = pressure fluctuation level in a frequency band of width Δf
T_c = nondimensional time scale, D/U_e
T_e = nondimensional period of oscillation, $1/T_c f$
U = velocity in the longitudinal direction, m/s
U_τ = $\sqrt{\tau/\rho}$
U_+ = U/U_τ
X, Y = nondimensional coordinates, x/D and y/D
x, y = Cartesian coordinates in the longitudinal and the transverse directions
Y_+ = law-of-the-wall coordinate, yU_τ/ν_w
Δf = bandwidth of Fourier analysis
ΔL = longitudinal distance between two cavities
α = ratio of time lag of pressure emission at trailing edge of the cavity and T_e
γ = ratio of specific heats, 1.4
δ = thickness of boundary layer
δ^* = displacement thickness of boundary layer
Θ = momentum thickness of boundary layer
μ = viscosity
ν = kinematic viscosity, μ/ρ
ρ = density
τ = shear stress
ω = angular frequency

Subscripts
e = freestream flow condition
w = wall condition

Introduction

CAVITIES have been studied extensively in the past due to their necessary existence on aircraft. Cavities may also be employed by design as flow control devices. Due to the characteristics of flows over cavities, studies have been undertaken in laboratories in attempts to understand flow phenomena such as separation,[1,2] heat transfer,[2,3] etc. Cavities may generate self-sustained oscillations under a wide range of flow conditions.[4-13] This self-sustained oscillation could be detrimental to the aerodynamic performance of an aircraft, its instrumentation, and the structure. Often cavities do not appear in isolation,[14,15] and it is the purpose of this paper to examine some of the effects of cavity-on-cavity interaction, both with respect to the temporal mechanisms and with respect to the time-mean behavior. The time-mean characteristics of the developing shear layer are considered important due to the effect on the drag of the cavities and due to the influence on the downstream aerodynamic components. Two types of cavities in which the oscillatory mechanisms differ are examined here. For the purposes of this paper, we defined the cavities examined as type A and type B. The time-mean flow over the cavities examined in this study is of "open" type[1,2] where the separated shear layer reattaches onto the downstream face of the cavity instead of the floor of the cavity.

The type A cavity oscillates in a manner that has been described by Rockwell and Naudascher[10] as a fluid-resonant phenomenon. In this class of cavities, flow-induced oscillations are influenced by resonant "wave" effects.[5] The characteristic of flow-induced oscillations in a resonator is that the shear layer at the orifice produces eddies that grow as they are convected across the cavity gap. If the growth rate and the convection velocity take the proper values, the eddy grows to fill the gap. In this manner, the eddy that has developed creates a compression in the cavity. The compressed fluid then ejects the eddy into the mainstream flow, and a new eddy develops in the gap. The oscillation, if it occurs, is therefore dominated by transverse modes, and the level of the pressure fluctuations is relatively small. An interferogram of the flow in an isolated type A cavity of the geometry tested here is shown in Fig. 1. A power spectral density plot of the surface pressure fluctuation measured on the floor of the aforementioned type A cavity is given in Fig. 2. The type A cavity flows investigated here exhibit some characteristics of both fluid-resonant and fluid-dynamic oscillations under certain conditions.[13] The

Presented as Paper 90-3087 at the AIAA 8th Applied Aerodynamics Conference, Portland, OR, Aug. 20–22, 1990; received Sept. 14, 1990; revision received June 26, 1991; accepted for publication Aug. 26, 1991.

*Research Assistant, Department of Engineering; currently at City University, Department of Mechanical Engineering and Aeronautics, Northampton Square, London EC1V 0HB, England, UK. Member AIAA.

†Rolls Royce Fellow, Wolfson College. Member AIAA.

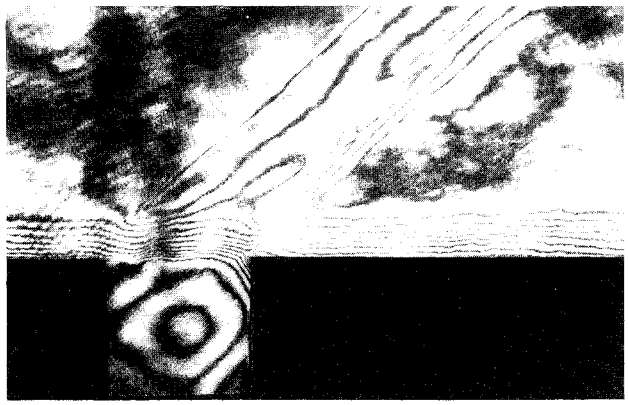

Fig. 1 Absolute holographic interferogram of type A cavity flow (L/D = 1) at M_e = 1.5.

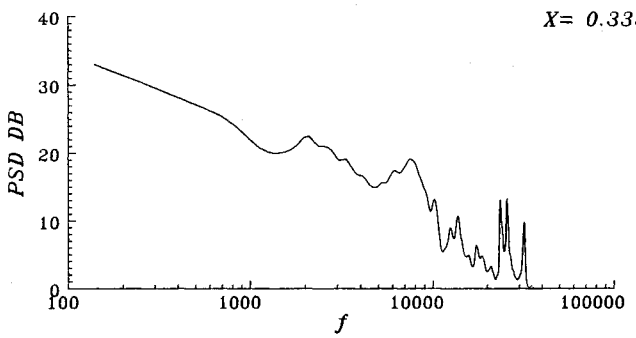

Fig. 2 Power spectral density of surface pressure in the L/D = 1 cavity at M_e = 1.5.

flow oscillation shown in Fig. 1 is dominated by dual modes at 23.4 and 25.7 kHz. As the length of the cavity increases, the transverse oscillation vanishes, and an oscillation based on a longitudinal mechanism appears. We call a cavity that oscillates with this mechanism a type B cavity.

The type B cavity oscillates with a mechanism that is attributed to the feedback of small disturbances on the downstream face of the cavity.[6] The disturbances propagate upstream to form a closed loop by influencing the shedding of the vortices. Based on this theory, semiempirical formulas[6,7] for the frequency of the oscillation were proposed, and practical means to attenuate the disturbances were introduced. This mechanism has been classified as a fluid-dynamic phenomenon by Rockwell and Naudascher. Recently, through flow visualization using holographic interferometry and computational study by solving the Navier-Stokes equations,[12,13] new flow features were observed, including the continuous shedding of vortices from the leading edge inside the cavity. A large vortex exists near the downstream face of the cavity. This vortex is called the trailing-edge vortex. The trailing-edge vortex moves in the transverse direction (i.e., y direction), controlling the inflow of mass and momentum into the cavity at the trailing edge. The size of this vortex is characterized by the depth D of the cavity. The trailing-edge vortex is constantly replenished by the series of vortices shed from the leading edge. The flow environment inside the cavity is thus determined by these vortices. The existence of the longitudinal oscillation is affected by a number of factors, including the cavity geometry, the state of the approaching boundary layer, Mach number, and Reynolds number. Linear stability theory indicates that this longitudinal mode of oscillation will not occur beyond Mach 2.7 because the shear layer is then stable. The length-to-depth ratio of the cavity also plays an important part in determining the characteristics of this longitudinal oscillation. As the length of the cavity is increased, turbulent dissipation in the shear layer ultimately damps the large-scale disturbances. Figure 3 shows an interferogram of the flow in an isolated oscillating cavity of the geometry tested in the following section. The oscillatory environment in the cavity is given by a power spectral density plot in Fig. 4. The flow is seen to be dominated by a single longitudinal mode at 5.9 kHz.

Previous investigations have shown that the cavity can exercise a considerable influence on the external flowfield.[14,15] In the present study, supersonic flows over two cavities in tandem were experimentally investigated. This study followed earlier investigations on a number of single cavity configurations, which included extensive experimental tests on cavities of different lengths at Mach 1.5, 2.5, and 3.5. The influence of a type A cavity on the oscillatory behavior of a type B cavity and vice versa is studied here. In addition the influence of the spacing between the two cavities is studied.

Test Arrangement

The Cambridge University Engineering Department supersonic wind tunnels were used. The tunnel working section is 1219 mm long, 279 mm high, and 114 mm wide. A half-liner configuration with interchangeable nozzle blocks was used. Each of the tunnel's side walls was equipped with a 203-mm diam optical window for spark schlieren and holographic interferometry. The cavities were mounted on the tunnel center line, on the half-liner section.[16] Each cavity had a depth of 15 mm. The length-to-depth ratio of the type A cavity was one and of the type B cavity was three. Three tandem cavity combinations were tested in the present study: a type A-type A configuration, a type B-type A configuration, and a type B-type B configuration. The distance between the cavities was varied from 15 to 95 mm. A typical type B-type A configuration is shown in Fig. 5. A Cartesian coordinate system is defined in Fig. 5, where the positive x axis refers to the streamwise direction, the positive y axis is defined parallel to the cavity upstream face and is positive toward the freestream, and the z axis refers to the spanwise direction. Pressure tappings, thermocouples, and miniature pressure transducers

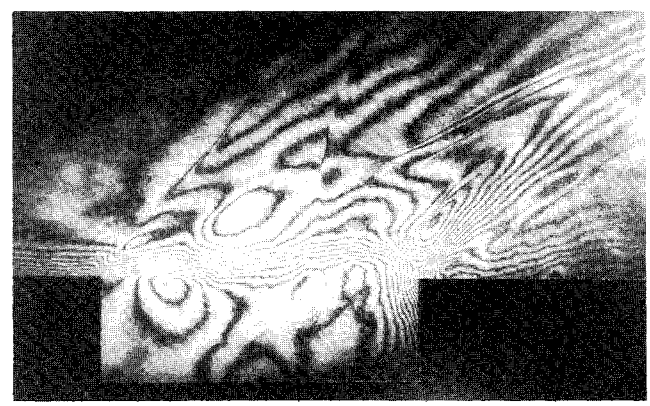

Fig. 3 Absolute holographic interferogram of type B cavity flow (L/D = 3) at M_e = 1.5.

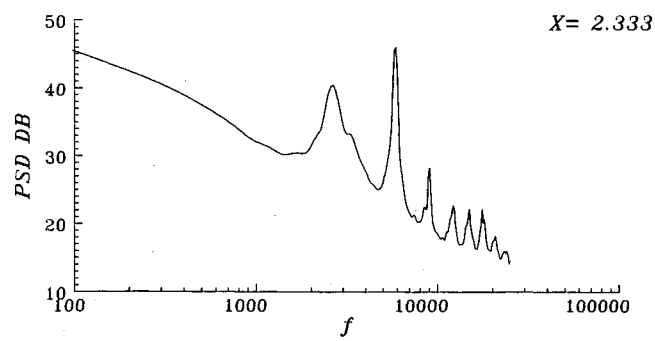

Fig. 4 Power spectral density of surface pressure in the L/D = 3 cavity at M_e = 1.5.

were inserted on the model surface. All measurements were within an 18-mm wide strip along the model center line. Although, the flowfield was observed to exhibit some three-dimensional characteristics, these were not found to affect the measurements severely.[11,13] Measurements made included time-mean and time-dependent surface pressures, total pressure traverses, spark schlieren photography, and holographic interferometry.

The time-mean surface pressures were measured from pressure tappings of 0.25-mm diam by way of a computer-controlled Scanivalve data acquisition system. The time-dependent surface pressures were sampled using Kulite XCQ-062-25A transducers. The sampling frequency was 70 kHz and the analysis bandwidth 68 Hz. Pitot pressure measurements were made using a steel pitot tube with a flattened head, 0.076 mm high. Holographic interferograms were recorded using a JK 2000 series, Q-switched ruby laser with a maximum output energy of 0.35 J per pulse. Both absolute and differential interferograms were made to examine the instantaneous density field and the temporal behavior of the density field.[17]

The turbulent boundary layer approaching the leading edge of the cavity was measured at each Mach number by both total pressure traverses and holographic interferometry. The boundary-layer characteristics from the pitot pressure survey are shown in Table 1. The oncoming boundary-layer thickness of the Mach 3.5 flow is 5.0 mm based on holographic interferometry. Skin friction was estimated using the logarithmic law of the wall proposed by Winter and Gaudet.[18] The skin friction coefficients of the oncoming boundary layer were also shown in Table 1.

Experimental Results

Type A Cavity Preceded by a Type A Cavity

The supersonic flow over a type A cavity is not altered significantly by a preceding type A cavity in terms of the basic flow features. The interferograms shown in Fig. 6 reveal no major changes in the flow over the second cavity. The single dominant vortex of the single type A cavity flow is clearly observed at Mach 1.5. The existence of this type of vortex flow inside the cavity is well established.[11,12,19] Analysis of the interferometric fringes in Fig. 6a, assuming constant static temperature inside the cavity, corresponds closely to the pressure distribution observed in Fig. 7a. Only a moderate increase of the boundary-layer thickness downstream of the tandem cavity configuration was observed. At Mach 1.5, the single vortex remains fairly symmetric in the second cavity. The flow in both cavities can be seen to be oscillatory as is shown by the broken structure in the density contours over the cavities. At Mach 2.5, the transverse oscillations[13] present in both cavities are revealed by the temporal density fields. A close look at the density contours shows that the waves above the second cavity are weakened by the shear layer. This is illustrated by the wider spacing observed between consecutive fringes. The different phase of the oscillation in each cavity is shown by the density contour patterns in the two cavities at Mach 2.5. At

Table 1 Boundary layer characteristics approaching the cavities

M_e	δ	δ^*	Θ	H	C_f
			Type A-type A		
1.5	4.13	0.864	0.384	2.24	0.00187
2.5	4.14	1.29	0.316	4.08	0.00141
			Type B-type A		
1.5	4.11	0.877	0.390	2.25	0.00172
2.5	4.22	1.33	0.333	4.02	0.00138
			Type B-type B		
1.5	4.31	0.979	0.431	2.28	0.00158
2.5	4.19	1.32	0.329	4.03	0.00139

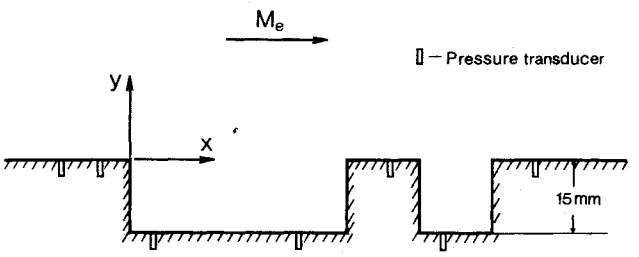

Fig. 5 Schematic of a typical test configuation.

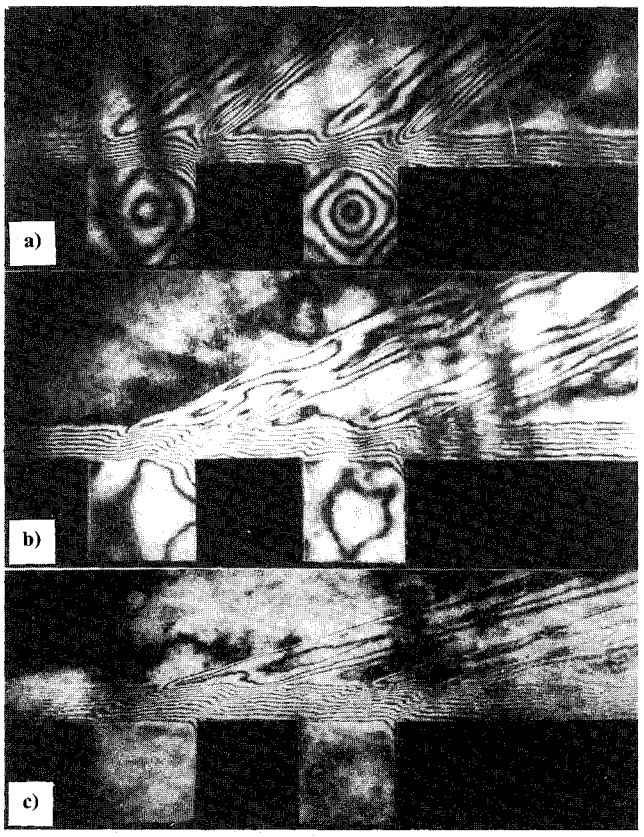

Fig. 6 Absolute holographic interferograms of type A-type A tandem cavity flows with $\Delta L = 1$ at a) $M_e = 1.5$, b) $M_e = 2.5$, and c) $M_e = 3.5$.

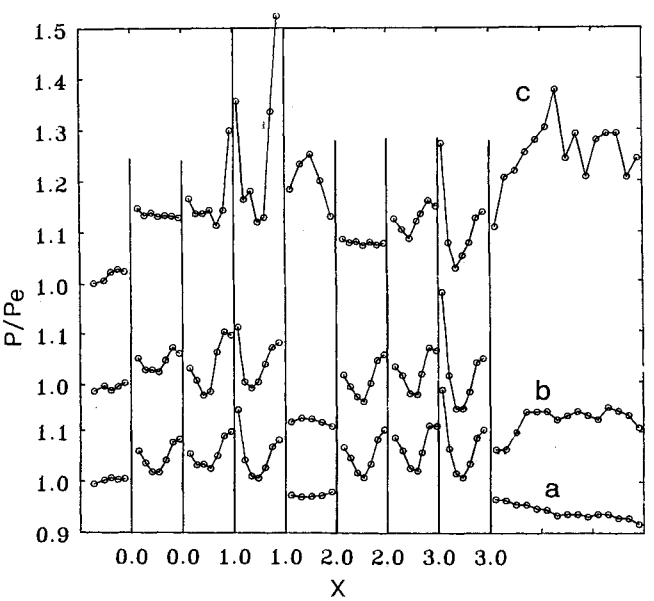

Fig. 7 Time-mean surface pressures of type A-type A tandem cavity flows with $\Delta L = 1$ at a) $M_e = 1.5$, b) $M_e = 2.5$, and c) $M_e = 3.5$.

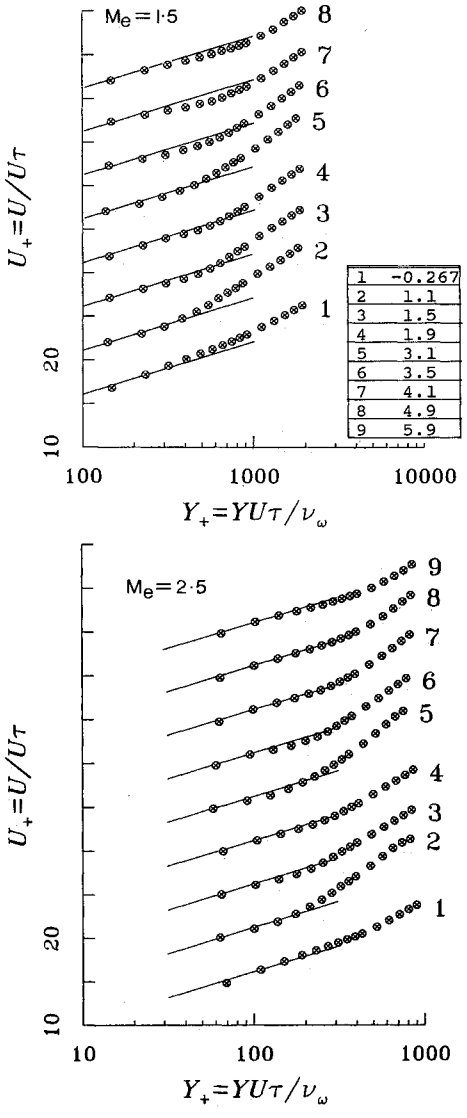

Fig. 8 Velocity profiles of boundary layer of flows over a type A-type A tandem cavity with $\Delta L = 1$.

Mach 3.5, both interferometry and spark schlieren indicate that the flow is stable in both cavities.

Time-mean surface pressure measurements were made with various distances between the two cavities, ranging from $1D$ to $7D$. At Mach 3.5, the high pressure near the downstream corner of the single cavity, due to the shear layer impingement, is not observed in the second cavity (Fig. 7). The cavity surface is unfolded to show the pressure distributions in Fig. 7 (and similarly in Figs. 11 and 18). The values shown plotted with an x-axis value of 0 represent the pressures on the upstream face of the cavity, and those with an x-axis value of 1 represent the pressures on the downstream face of the cavity. The pressure on the upstream face of the second cavity is lower than that of the single cavity. This low pressure is induced by momentum diffusion in the shear layer. At Mach 1.5 and 2.5, the influence of the type A cavity on the following type A cavity is quite different from that at Mach 3.5. The pressure near the downstream corner of the second cavity is increased due to the presence of the preceding cavity. This increased pressure, even on a small scale, is thought to be a result of the increased oscillatory level that modifies the mean impingement position on the downstream face of the second cavity. Also at this Mach number the pressure on the upstream face of the second cavity falls in comparison with that of the upstream cavity. The shear layer survey does not indicate any significant changes in the boundary-layer structure. Overall, there is only a slight increase of the thickness and shape factor. The law of the wall is seen to represent the velocity profile well (Fig. 8).

The time-dependent surface pressures on the floor of the cavity indicate that the oscillatory frequencies are not modified in the second cavity. However, certain modes are altered (Fig. 9). At Mach 1.5, the dual modes at 23.4 and 25.7 kHz in the second cavity ($X = 2.33$) as shown by the power spectral

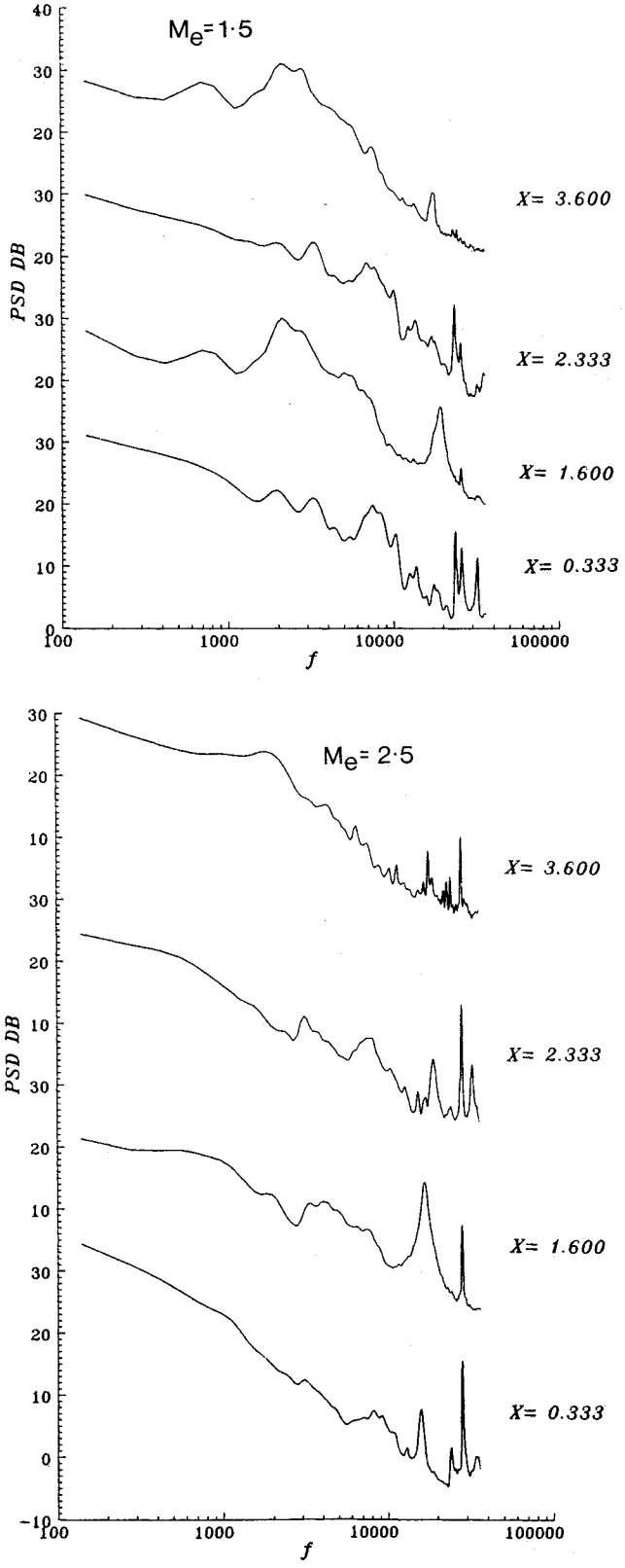

Fig. 9 Power spectral densities of surface pressure fluctuation of flows over a type A-type A tandem cavity with $\Delta L = 1$.

plots demonstrate that the flow is still controlled by both the transverse mode and the longitudinal mode in the single cavity. The high frequency mode at 31.8 kHz disappears. This is suppressed by the shear layer. The longitudinal mode at 25.7 kHz is also detected downstream of the trailing edge of the first cavity (X = 1.6), along with a broadband mode at 19.1 kHz, this latter being due to the separation shock wave motion on the cavity. At Mach 2.5, the influence of the first cavity on the oscillation in the second cavity through the unsteady shear layer is much clearer. The dominant oscillatory mode at 28 kHz is observed in both cavities, as well as downstream after each cavity. The mode due to the shock wave seen at 16.7 kHz is not detected downstream of the second cavity. This is again thought to be damped by the thickened shear layer. Also at Mach 2.5 the weak longitudinal mode at 32.4 kHz is slightly amplified in the second cavity. This is probably due to the modified shear layer, as it is not observed in the first cavity.

Type B Cavity Preceded by a Type B Cavity

In the single cavity study,[13] it was found that a strong longitudinal oscillation was present in a type B cavity at Mach 1.5

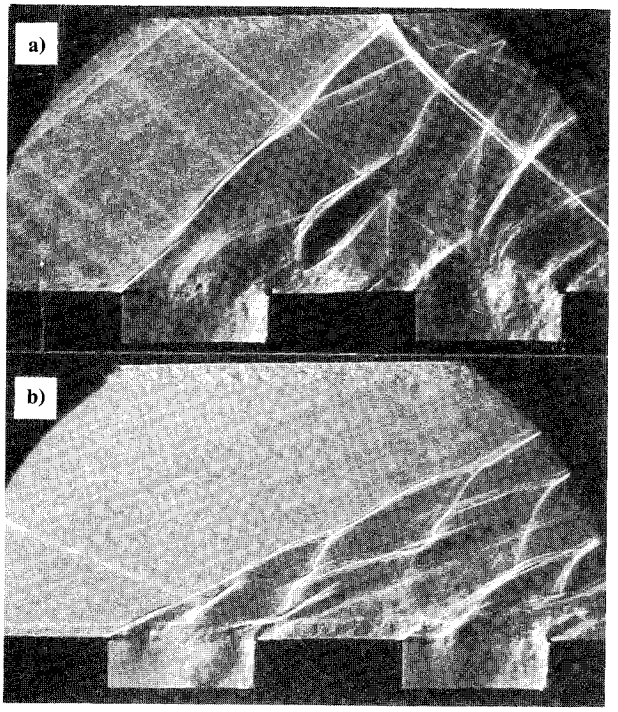

Fig. 10 Spark schlieren visualizations of type B-type B tandem cavity flows with ΔL = 3 at a) M_e = 1.5 and b) M_e = 2.5.

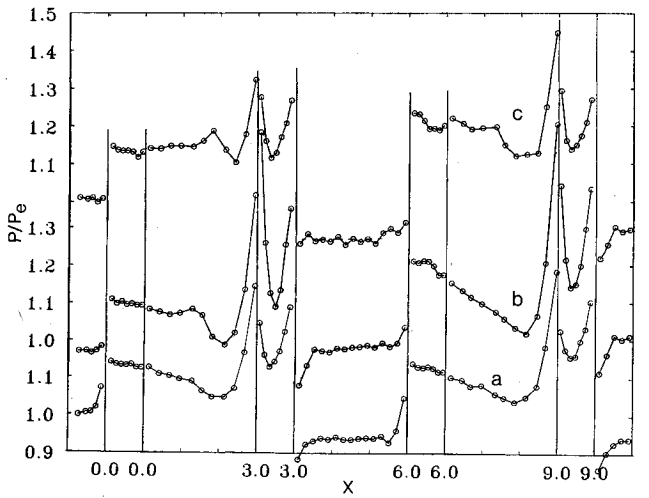

Fig. 11 Time-mean surface pressures of type B-type B tandem cavity flows with ΔL = 3 at a) M_e = 1.5, b) M_e = 2.5, and c) M_e = 3.5.

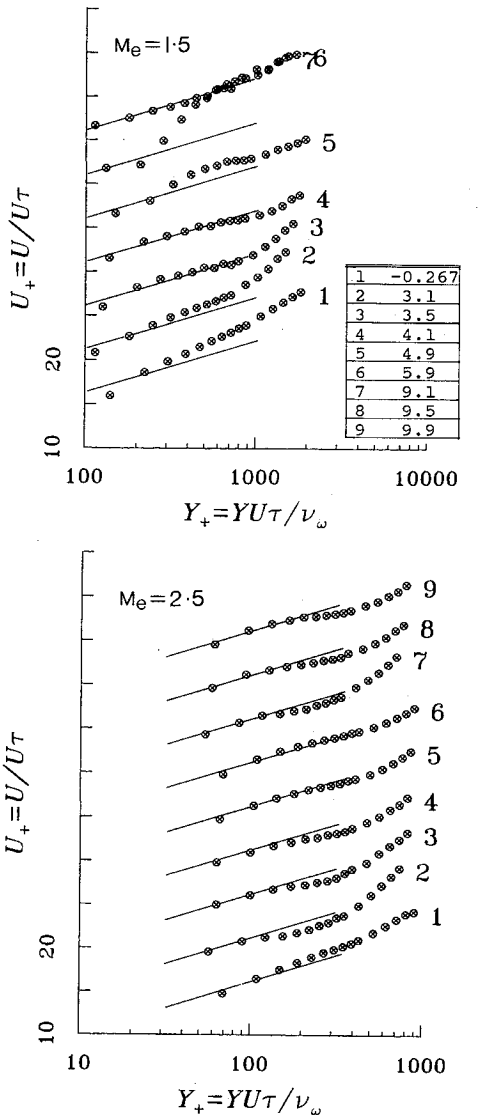

Fig. 12 Velocity profiles of boundary layer of flows over a type B-type B tandem cavity with ΔL = 3.

and 2.5 and further that the flow is stable at Mach 3.5. When the type B cavity is preceded by another type B cavity, both schlieren observation (Fig. 10) and holographic interferometry do not reveal significant changes in the structure of the oscillatory flow at Mach 1.5 and 2.5. It seems that the effect of the preceding cavity is mainly to set the phase of the oscillation in the succeeding cavity. The shear layer thickness increases sharply after the first cavity and continues to do so after the second.

The time-mean surface pressure in the second cavity is not severely modified by the presence of the first cavity (Fig. 11). All of the basic features of the flow observed for a single type B cavity are retained. Only a moderate increase of the pressure near the downstream corner is observed. The reattached boundary layer after each cavity, however, shows a "wake-like" structure at Mach 1.5 and 2.5 (see, for example, Fig. 12). An inflection point appears in the velocity profile downstream of each cavity. The increased mixing level in the shear layer caused by the oscillation in the cavity increases the boundary-layer thickness significantly.

From Fig. 13, we can observe that the dominant oscillatory modes at 5.9 kHz at Mach 1.5 and 10.0 kHz at Mach 2.5 are present in the second cavity. On the spacing between the two cavities, the dominant (second), third, and fifth modes are detected at Mach 1.5. The broadband mode at 18.4 kHz due to the shock wave motion at the leading edge of the cavity is

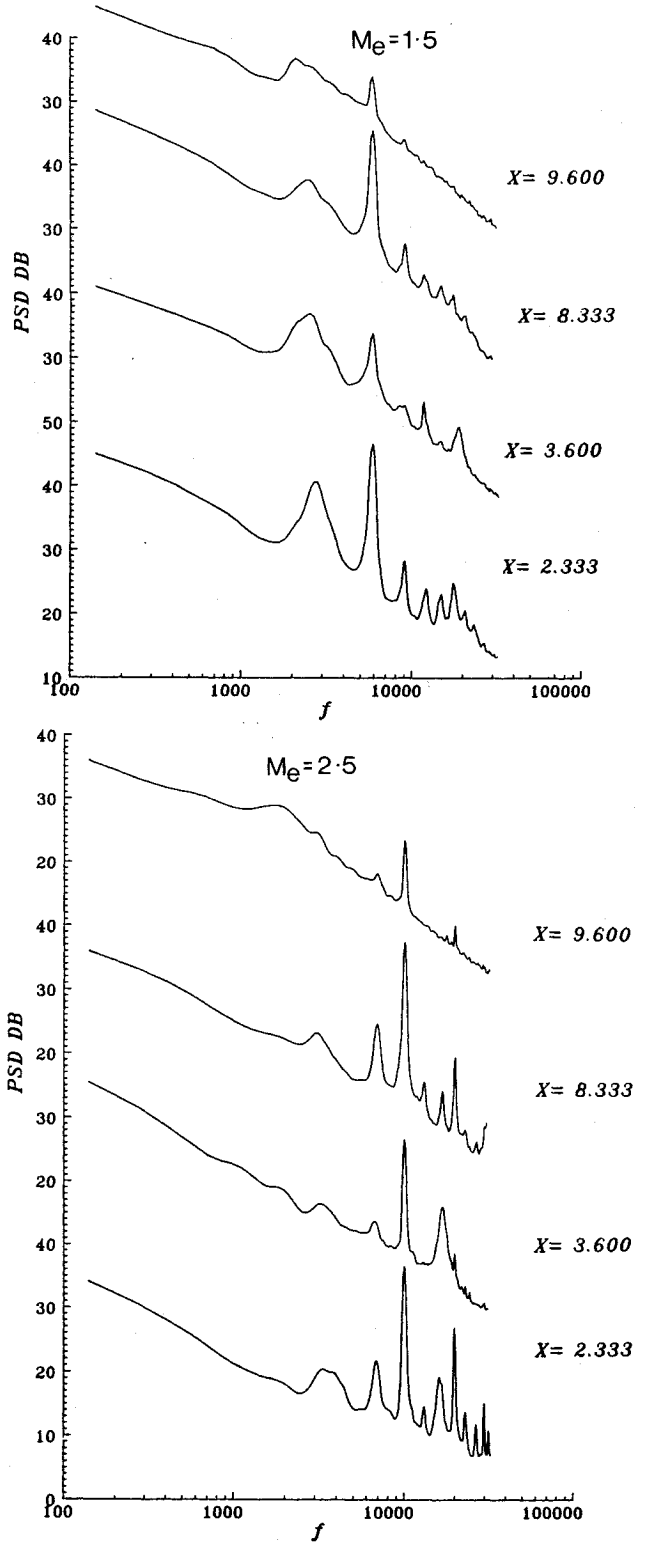

Fig. 13 Power spectral densities of surface pressure fluctuation of flows over a type B-type B tandem cavity with $\Delta L = 3$.

damped by the thick shear layer downstream of the first cavity. Downstream of the second cavity only the dominant mode is observed. At Mach 2.5, the broadband mode at 16.7 kHz due to the leading-edge shock wave is still present downstream of the first cavity but is not observed after the second cavity.

Cross-covariance analysis of the time-dependent surface pressure data was undertaken. From this one can calculate the time lag between events at two sampling positions and hence the phase difference between the pressure fluctuations. Except for the case in which the time-dependent surface pressures are sampled on the floor of the cavity, the time lag can be interpreted as the time it takes for a large vortical structure[12,13] to be convected from one measuring station to another. In the present case, all of the time lags are calculated against a reference time at $X = 2.33$ in the first cavity. At Mach 1.5, the time between two positions ($X = 3.6$ and 9.6), the first being downstream of the first cavity and the second being downstream of the second cavity, is 8.13 T_c. This implies a convective speed for the disturbance of 0.74 U_e. At Mach 2.5, this convective speed is found to be 0.70 U_e. At Mach 1.5, the time lag between two positions ($X = 2.33$ and 3.6), the first being on the floor of the first cavity and the second being downstream of the trailing edge of the first cavity, is 1.75 T_c. For the second cavity, the corresponding time lag is 0.88 T_c. At Mach 2.5, at the same sampling positions, the time lag is 0.9 T_c for the first cavity and 0.25 T_c for the second cavity.

Type A Cavity Preceded by a Type B Cavity

Figure 14 shows a typical spark schlieren photograph of the flow at Mach 1.5. Figure 15 shows absolute and differential holographic interferograms. The most prominent feature of the flow over this configuration is the strong longitudinal oscillation present in the second cavity. It is known from single cavity studies[10] that the longitudinal oscillation of a single cavity is characterized by the dimensions of the cavity. Thus the flow oscillation in the type A cavity should be dominated by a higher frequency mode than that of the type B cavity for the present test configurations. However, from observation in

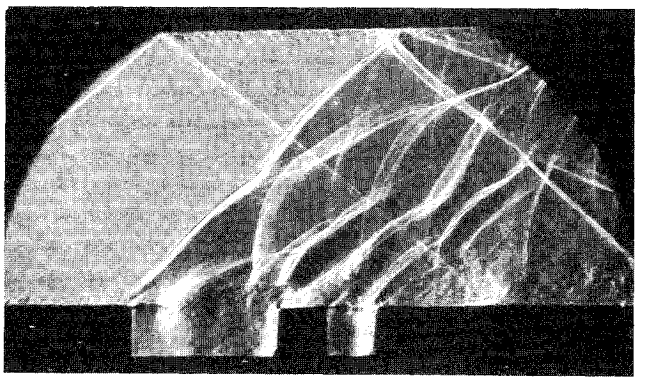

Fig. 14 Spark schlieren flow visualization of an $M_e = 1.5$ flow over a type B-type A tandem cavity with $\Delta L = 1$.

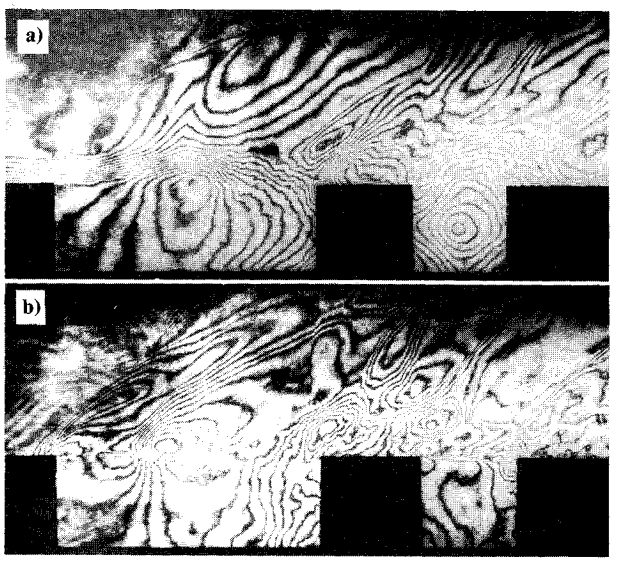

Fig. 15 Holographic interferograms of type B-type A tandem cavity flows at $M_e = 1.5$; a) absolute and b) differential with $\Delta t = 100$ μs and $\Delta L = 1$.

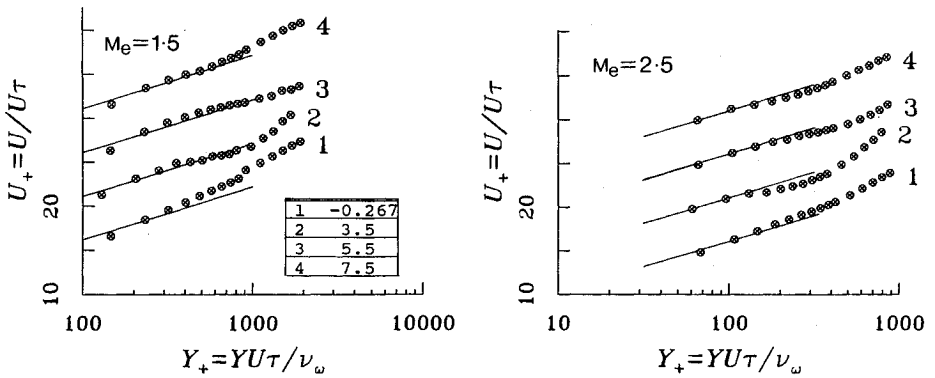

Fig. 16 Velocity profiles of boundary layer of flows over a type B-type A tandem cavity with $\Delta L = 3$.

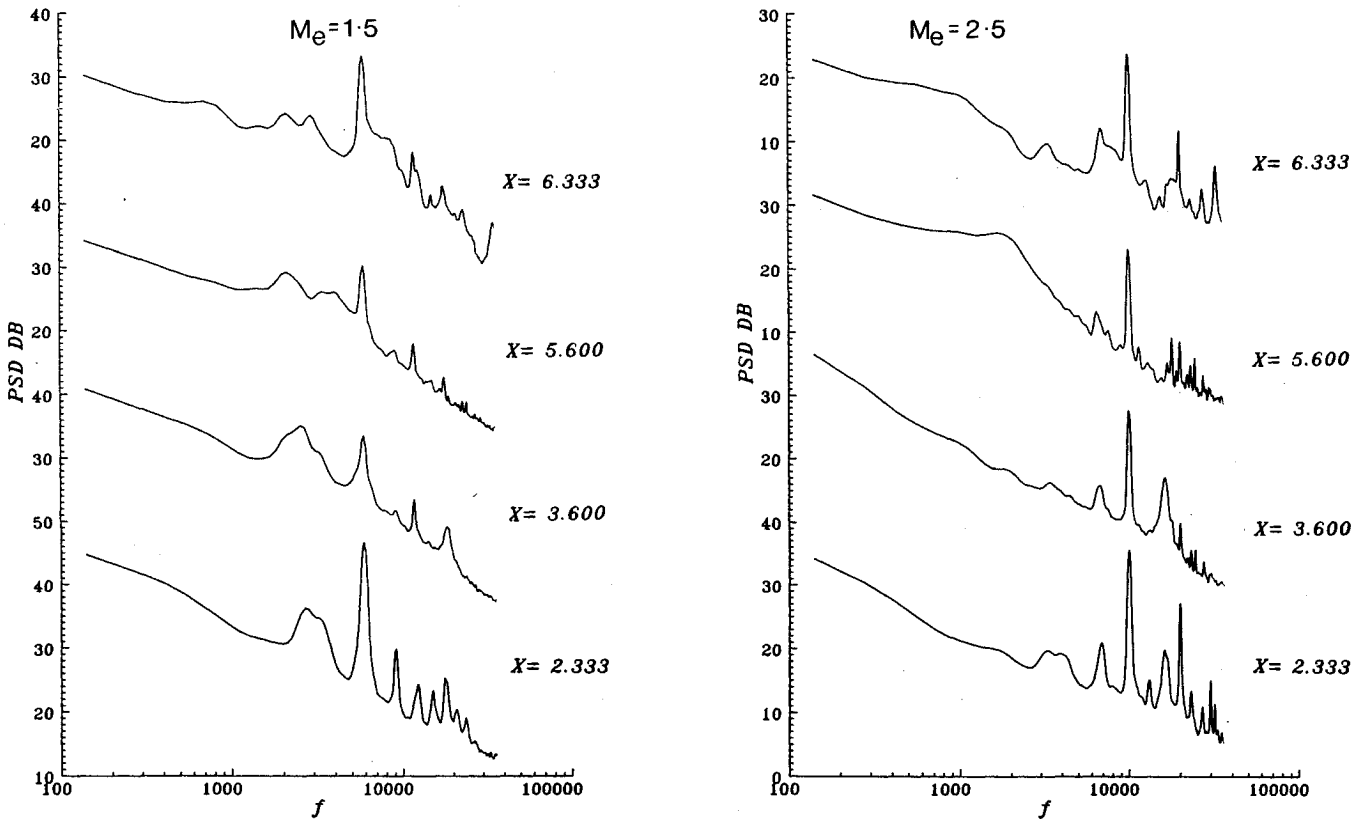

Fig. 17 Power spectral densities of surface pressure fluctuation of flows over a type B-type A tandem cavity with $\Delta L = 3$.

Fig. 14, the temporal pressure waves above the second cavity, in this tandem cavity configuration, indicate that the oscillation in the second cavity is dominated by a mode with a comparable wavelength to that of the preceding type B cavity. The interferograms in Fig. 15 show the extent to which the second cavity flow is affected (compare with Fig. 1). The fringe spacing inside the type A cavity is much closer than that for a solitary type A cavity. The large vortical structures generated in the shear layer over the first cavity by the longitudinal oscillation are convected downstream.

At both Mach 1.5 and 2.5, the turbulent boundary layer is significantly modified downstream of the first cavity as is shown by the semilogarithmic velocity profiles of boundary layer of Fig. 16. The boundary layer shows wakelike characteristics. An inflection point is detected in the velocity profiles of the reattached boundary layer. The changes in the flow structure observed visually in Figs. 14 and 15 are verified through time-dependent surface pressure measurements. Power spectral densities at Mach 1.5 and 2.5 are shown in Fig. 17. The oscillation in the type A cavity is modified by the preceding type B cavity. At Mach 1.5, the oscillation in the type A

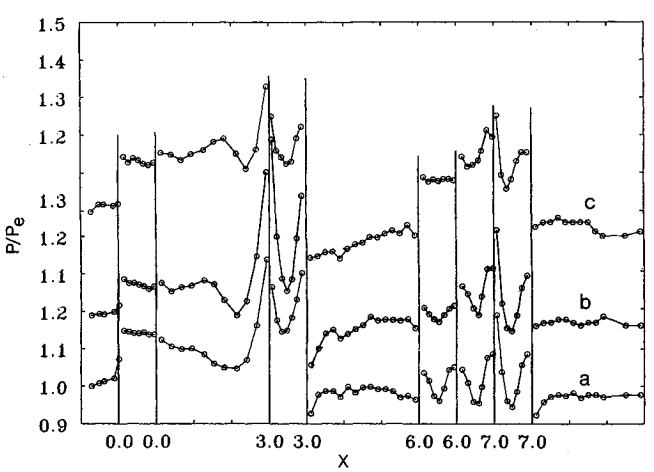

Fig. 18 Time-mean surface pressures of type B-type A tandem cavity flows with $\Delta L = 3$ at a) $M_e = 1.5$, b) $M_e = 2.5$, and c) $M_e = 3.5$.

cavity is dominated by a mode at 5.9 kHz, rather than the dual modes at 23.4 and 25.7 kHz for the isolated cavity flow (see Fig. 2). The dominant mode is that of the leading cavity. Similar results are observed at Mach 2.5. The unsteady surface pressure measurements downstream of each cavity again indicate the convection of large-scale disturbances by the shear layer. This can also be observed in the differential holographic interferogram (Fig. 15b).

Figures 18a–18c show, respectively, time-mean surface pressures for Mach numbers 1.5, 2.5, and 3.5. At Mach 3.5, the time-mean surface pressure near the downstream corner of the second cavity is reduced from 1.6 P_e for the single cavity flow to 1.2 P_e as the distance between the two cavities increases from 1D to 5D. Since the recompression on the downstream face is a major influence on the total drag in the cavity, this is expected to lead to a reduction in the drag coefficient of the cavity. When the type B cavity is oscillating, the effect is different. In this case, there is a substantial increase in the time-mean pressure on the downstream face of the type A cavity. The effect of the first cavity on the flow behavior in the second reduces as the separation between the cavities increases.

Discussion and Conclusions

A supersonic flow over a single cavity is characterized by many features, for example, leading-edge and trailing-edge vortices in the cavity, the diffusion of momentum and turbulent dissipation in the shear layer, the shear layer impingement on the downstream face of the cavity, recompression of the flow, and oscillation. These features are likely to be influenced by Mach number, cavity geometry, and the state of the oncoming boundary layer. When a cavity is preceded by another cavity, the flow over the cavity can be strongly affected by the preceding cavity through modifications to the shear layer. When the shear layer is thick, as in the present study, the influence of the first cavity is significant, and in addition, due to the change in the shape factor of the shear layer approaching the second cavity, it is possible that a significant effect on the first cavity may be observed due to the presence of the second cavity. However, the interaction between two cavities in a tandem cavity configuration depends on the types of cavities involved.

In the theoretical description of the longitudinal oscillation,[6,7] disturbances generated near the leading edge of the cavity are convected downstream. Upon reaching the trailing edge of the cavity, pressure waves are radiated inside the cavity. In these theories, to predict the frequencies it is necessary to introduce an empirical parameter α to bridge the difference between theory and experiment.[7] This parameter represents a phase shift in Rossiter's formula.[6] In the present study, the vortical structures in the shear layer are observed to be of considerable size compared with the shear layer thickness. When a vortex reaches the trailing edge of the cavity, the emission of the pressure wave is not instantaneous, and hence a time lag exists.[12] In addition, the relatively the large size of the vortical structure generates a broadband pressure pulse.

In this study, the time lag is estimated through cross-covariance analysis of the time-dependent surface pressures at different positions; α is defined as the ratio of the time lag between the arrival of the vortical structure and the pressure wave emission and the period of oscillation T_s. The value of α is found to be 0.36 at Mach 1.5 and 0.32 at Mach 2.5 for the first cavity of a type B-type B tandem cavity configuration with the distance between the two cavities being 3D. For the second cavity in this test configuration, the value of α is 0.89 at Mach 1.5 and 0.56 at Mach 2.5. The increase in α is probably due to the stretching of the vortical structures as is observed in the differential holographic interferograms. There are discrepancies between the value of α found in the present study and that given by Rossiter (0.24). The convection velocity of the disturbances (0.7–0.75 U_e) is also found to be different from that given by Rossiter (0.57 U_e). In addition, it was observed in Zhang and Edwards[12] that there is an effective time lag between the arrival of pressure pulse at the leading edge and the full development of a leading-edge vortex. These factors will have to be taken into consideration in any theoretical description of the frequencies and their phases observed here.

There is a fundamental difference between a stable tandem cavity flow and an oscillatory tandem cavity flow, regardless of the types of cavities involved. When the single cavity flow is stable, as at Mach 3.5 in the present study, the effect of the preceding cavity on the second cavity is clear. The shear layer impingement at the trailing edge of the second cavity is weakened due to the increased level of the momentum diffusion across the shear layer. This leads to a drop of the surface pressure on the downstream face of the cavity, and subsequently we expect a reduction in the drag coefficient. When the flow over the tandem cavity configuration is oscillatory, the interaction between the two cavities is different. When the cavities oscillate in a transverse mode, such as that in our type A-type A cavity configuration at Mach 1.5 and 2.5, the effect of the preceding cavity is to modify the oscillation in the second cavity by damping the high frequency modes and to enhance the dominant mode. The high frequency modes are damped through turbulent dissipation in the thickened shear layer approaching the second cavity. If flows in both cavities oscillate in a longitudinal mode, such as those in a type B-type B tandem cavity configuration, the disturbance generated by the first cavity is convected downstream and is amplified by the second cavity. This modification to the flowfield in the second cavity increases the influence of shear layer impingement on the downstream face of the second cavity and increases the drag coefficient of the cavity. The natural oscillatory modes in the second cavity are not changed but will be phase locked with the convected disturbances.

When a type B cavity precedes a type A cavity, the flow oscillation in the type A cavity is completely modified. In isolation, the type A cavity oscillates in a transverse mode, but in the type B-type A cavity configuration the type A cavity is dominated by the oscillatory characteristics of the type B cavity. This is achieved through a modified unsteady turbulent boundary layer approaching the second cavity with both increased boundary-layer thickness and changed velocity profile, so that a hydrodynamically unstable shear layer approaches the second cavity. The large-scale vortical structures are observed to be present over the second cavity and are convected downstream by the shear layer. The natural oscillation in the second cavity is weak and is suppressed in favor of the longitudinal modes generated in the type B cavity. The internal vortex in the type A cavity is strengthened. The combination of these effects could lead to a substantial increase in the drag of the second cavity.

Acknowledgment

This work was funded by the Procurement Executive, Ministry of Defence, United Kingdom.

References

[1]Charwat, A. F., Roos, J. N., Dewey, F. C., Jr., and Hitz, J. A., "An Investigation of Separated Flows—Part I: The Pressure Field," *Journal of the Aerospace Science,* Vol. 28, No. 6, June 1961, pp. 457–470.

[2]Charwat, A. F., Dewey, F. C., Jr., Roos, J. N., and Hitz, J. A., "An Investigation of Separated Flows—Part II: Flow in the Cavity and Heat Transfer," *Journal of the Aerospace Science,* Vol. 28, No. 7, July 1961, pp. 513–527.

[3]Thomann, H., "Measurement of Heat Transfer and Recovering Temperature in Regions of Separated Flow at a Mach Number of 1.8," Aeronautical Research Inst. of Sweden, Rept. 82, Bromma, Sweden, Nov. 1958.

[4]Krishnamurty, K., "Acoustic Radiation from Two-Dimensional Cutout in Aerodynamic Surface," NACA TN-3487, Aug. 1955.

[5]Plumblee, H. F., Gibson, G. S., and Lassiter, L. W., "A Theoretical and Experimental Investigation of the Acoustic Response of Cavi-

ties in an Aerodynamic Flow," Wright Air Development Division, WADD-TR-61-76, Wright-Patterson AFB, OH, March 1962.

[6]Rossiter, J. E., "Wind Tunnel Experiment on the Flow over Rectangular Cavities at Subsonic Transonic Speeds," British Aeronautical Research Council, ARC R&M 3438, London, UK, Oct. 1964.

[7]Heller, H., Holmes, G., and Covert, E., "Flow Induced Pressure Oscillations in Shallow Cavities," Air Force Flight Dynamics Lab., AFFDL-TR-70-140, Wright-Patterson, AFB, OH, Dec. 1970.

[8]Heller, H., and Bliss, D., "Aerodynamically Induced Pressure Oscillations in Cavities: Physical Mechanisms and Suppression Concepts," Air Force Flight Dynamics Lab., AFFDL-TR-74-133, Wright-Patterson AFB, OH, Feb. 1975.

[9]Hankey, W. L., and Shang, J. S., "Analysis of Pressure Oscillations in an Open Cavity," *AIAA Journal,* Vol. 18, No. 9, 1980, pp. 892–898.

[10]Rockwell, D., and Naudascher, E., "Review of Self-Sustaining Oscillations of Flow Past Cavities," *ASME Journal of Fluid Engineering,* Vol. 100, No. 2, June 1978, pp. 152–165.

[11]Rizzetta, D. P., "Numerical Simulation of Supersonic Flow over a Three-Dimensional Cavity," *AIAA Journal,* Vol. 26, No. 7, 1988, pp. 799–807.

[12]Zhang, X., and Edwards, J. A., "Computational Analysis of Unsteady Supersonic Cavity Flows Driven by Thick Shear Layer," *Aeronautical Journal,* Vol. 92, Nov. 1988, pp. 365–373.

[13]Zhang, X., and Edwards, J. A., "An Investigation of Supersonic Oscillatory Cavity Flows Driven by Thick Shear Layer," *Aeronautical Journal,* Dec. 1990, pp. 355–364.

[14]Degen, C. L., "Pressure Fluctuation Caused by the Flow Past Many Cavities," M.S. Thesis, Imperial College of Technology, London, UK, Sept. 1983.

[15]Edwards, J. A., and Zhang, X., "Some Aspects of Supersonic Flow over a Cavity Cascade," AIAA Paper 86-2025, Aug. 1986.

[16]Zhang, X., "An Experimental and Computational Investigation into Supersonic Shear Layer Driven Single and Multiple Cavity Flowfields," Ph.D. Thesis, Dept. of Engineering, Cambridge Univ., Cambridge, England, UK, 1987.

[17]Edwards, J. A., "Some Applications of the Temporal Properties of Holographic Interferometry," Rolls Royce Plc, Aeroelastic Research Rept. ARR 90306, Derby, England, UK, 1988.

[18]Winter, K. G., and Gaudet, L., "Turbulent Boundary-Layer Studies at High Reynolds Numbers at Mach Numbers Between 0.2 and 2.8," British Aeronautical Research Council, ARC R&M 3712, London, UK, Dec. 1970.

[19]Ghaddar, N. K., Korzak, K. Z., Mikic, B. B., and Patera, A. T., "Numerical Investigation of Incompressible Flow in Grooved Channels," *Journal of Fluid Mechanics,* Vol. 163, Feb. 1986, pp. 99–127.